Temperature dependence of brightness temperature difference of AVHRR infrared split window channels in the Antarctic

Gaku Kadosaki[1], Takashi Yamanouchi[1,2] and Naohiko Hirasawa[1,2]

[1] *Department of Polar Science, School of Mathematical and Physical Science,*
The Graduate University for Advanced Studies, Kaga 1-chome,
Itabashi-ku, Tokyo 173-8515
[2] *National Institute of Polar Research, Kaga 1-chome, Itabashi-ku, Tokyo 173-8515*

Abstract: One method to identify clouds from NOAA/AVHRR data is to use the difference in brightness temperature of infrared split window channels in the $10\,\mu$m region. Under the low temperature over the Antarctic continent in winter, it is necessary to detect a slight difference in brightness temperature. In this paper, we investigate the temperature dependence of the brightness temperature difference of channel 4 ($10.8\,\mu$m) brightness temperature (T4), and channel 5 ($12\,\mu$m) brightness temperature (T5) (T4–T5) of a cloud free scene.

T4–T5 is about 0℃ at low temperature around -80℃, and gradually increases up to a high of 1℃ at high temperature around 0℃. The rates of increase in T4–T5 were almost constant for T4 lower than -40℃. For T4 higher than -30℃, T4–T5 remains almost unchanged. For T4 between -40℃ and -30℃, T4–T5 increases rapidly.

In order to explain this temperature dependence, the contribution of water vapor and surface emissivity to the difference in brightness temperature was calculated from *in situ* data using the radiation code MODTRAN. The result is shown below. About the contribution of water vapor, at T4 lower than -25℃, T4–T5 was nearly zero. From about -25℃ to 0℃ of T4, T4–T5 increases up to near 0.6℃. On the other hand, when the surface emissivity difference between CH4 and CH5 was set to 0.01, T4–T5 increased in all temperature ranges. The rate of increase was almost constant. In the temperature range lower than -40℃, T4–T5 conformed to T4–T5 of satellite data.

1. Introduction

Satellite remote sensing is an indispensable tool for meteorological analysis; especially, tied closely to clouds, it is required in the Antarctic which has very few observing points. Since the presence of clouds in polar regions particularly has a significant impact on radiation balance of the earth (Yamanouchi and Kawaguchi, 1984; Curry *et al.*, 1996), it is important to obtain information on the cloud distribution in polar regions year round; however, it is difficult to obtain cloud distributions year round using visible and single infrared satellite data in high latitudes due to high albedo and low snow surface temperature, which makes the contrast between clouds and the snow surface small. A great deal of effort has been put into polar cloud detection from satellite passive measurements. There is a method to detect clouds from the difference between

AVHRR split window channels (Yamanouchi *et al.*, 1987). This method uses the distribution of the brightness temperature difference of channels 4 (CH4) and 5 (CH5) (T4–T5) against the brightness temperature of CH4 (T4). The distribution of pixels affected by cloud: the particle size, temperature and optical thickness. On the scatter diagram of T4–T5 against T4, pixels of the thin clouds distribute as archwise. The curve starts from the point for clear sky (as surface temperature), passes through points for each thickness, and then converges to the point for infinite thickness (cloud top temperature). The top of the arch (maximum value of T4–T5) is varies with particle size and temperature.

Recently, Yamanouchi *et al.* (2000) indicated that in some cloudy cases, the very small value of T4–T5 (1°C) and no arch on the scatter diagram are seen over inland Antarctica. Such a small value of T4–T5 makes it difficult to distinguish between cloudy and clear pixel areas. Considering these results, it is significant to clarify the characteristics of T4–T5 in a cloud free area. Thus, in this paper, we examine T4–T5 of a cloud free scene over inland Antarctica with satellite data, and discuss temperature dependence from calculation using *in situ* data and the radiation code "MODTRAN (Anderson *et al.*, 1995)".

2. Data and analysis

Advanced Very High Resolution Radiometer (AVHRR) data from the polar orbiting satellite NOAA-14 used in this study were received by the 38th Japanese Antarctic Research Expedition (JARE-38) at Syowa Station (the positions of stations are shown in Fig. 1). The AVHRR has five sensor channels: channel 1, 0.58–0.68 μm; channel 2, 0.725–1.10 μm; channel 3, 3.55–3.93 μm; channel 4, 10.3–11.3 μm; and channel 5, 11.5–12.5 μm. The instantaneous field of view (IFOV) of each channel is approximately 1.4 milliradians (mr), leading to a resolution at the nadir point of 1.1 km for a nominal altitude of 833 km (NOAA, 1998). The data were calibrated with the method prescribed by the National Oceanic and Atmospheric Administration (NOAA,
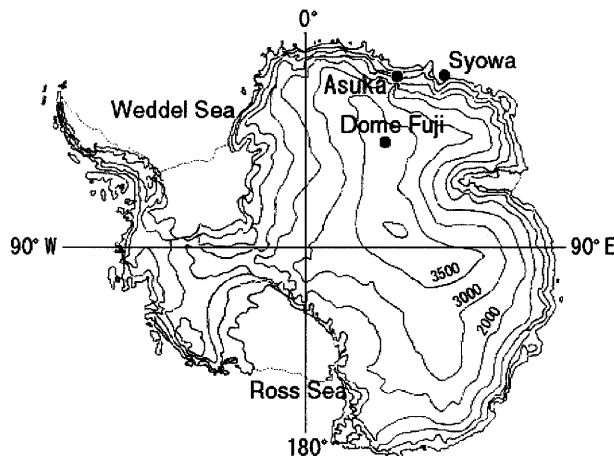

Fig. 1. *The positions of each station in the Antarctic.*

1988).

In this study, data set 1 for large areas shows schematically the temperature dependence of T4–T5 against T4 over a wide temperature range. Data set 2 explains the temperature dependence of T4–T5 against T4 in a narrow specific area with simple topography.

Data set 1 covers a wide and cloud free area in various seasons. We manually inspected visible (CH1) and infrared (CH4) images from March 1997 to February 1998, selected 5 passes on May 6, June 3, August 31, October 20 and November 19, 1997, and extracted five cloud free areas of inland Antarctica. The extracted areas, are square regions of about 500×1350 km to 1000×1350 km, and include various elevations and slopes. An example of the areas used is shown in Fig. 2. The square represents the portion used for analysis. For efficient calculation, 1 pixel was sampled out of every 4 pixels in the raw data to reduce the amount of data. Due to the limited brightness temperature resolution of the sensor, the data tend to have discrete values at low temperatures. Data over 4×4 pixel areas were averaged to reduce this effect.

Data set 2 is based on a specific area mainly around Dome Fuji Station. These data were extracted at times and in areas where the cloud amount was zero within three hours before and after the satellite pass from ground-based observation data obtained by
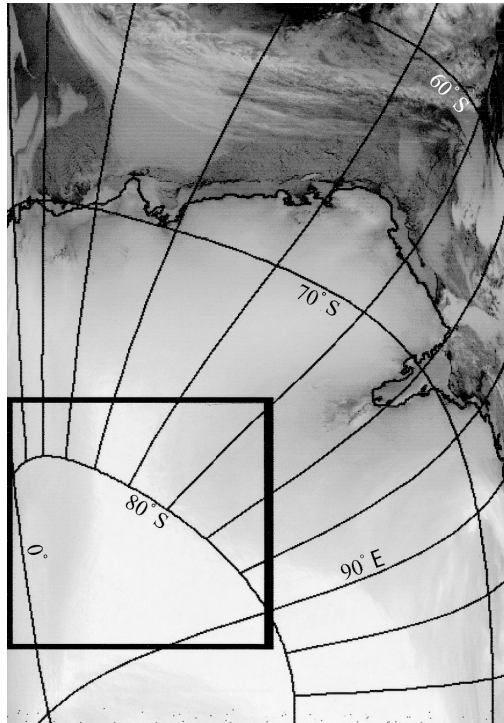

Fig. 2.   An example of the areas used for study on dependence of T4–T5 on T4 over an extensive cloud free surface.   This scene was created from the infrared data at about 13UT on October 20, 1997.   The square represents the portion used in the analysis.

JARE38 at Dome Fuji Station from 1997 to 1998 (Japan Meteorological Agency, 1999). The data area is a square of 64×64 pixels and is equivalent to 70×70 km. Data were averaged over 4×4 pixels to reduce discrete distribution as mentioned above.

3. Results and discussion

Figure 3 shows a scatter diagram of T4–T5 against T4 over a wide temperature range continuously, which was made from data set 1. Figure 3 indicates an increasing trend of T4–T5 versus T4. At very low T4, around $-80°C$, T4–T5 can be seen as $0°C$, T4–T5 increases at a fixed rate with the increase of T4 from $-80°C$, and reaches about $0.3°C$ at about $-40°C$. At T4 from $-40°C$ to $-30°C$, the rate of increase in T4–T5 becomes large, and at about $-30°C$, T4–T5 converges to about $1°C$; however, we cannot obtain a clear trend at T4 larger than $-30°C$ due to larger variation.

Figure 4 shows a scatter diagram of T4–T5 against T4 for the narrow specific area around Dome Fuji Station. Since this area is narrow, the data for each day have a temperature range of only $5°C$. We plot data on a diagram to indicate trend of temperature dependence. In addition to data set 2 at Dome Fuji Station, data from Syowa Station and another sampling area about 100 km north of Asuka Station were also used when the temperature was comparatively warm. We used ground-based observations at Syowa Station (Japan Meteorological Agency, 1999) as ground truth in clear conditions. The data near Asuka station were used to cover the range between
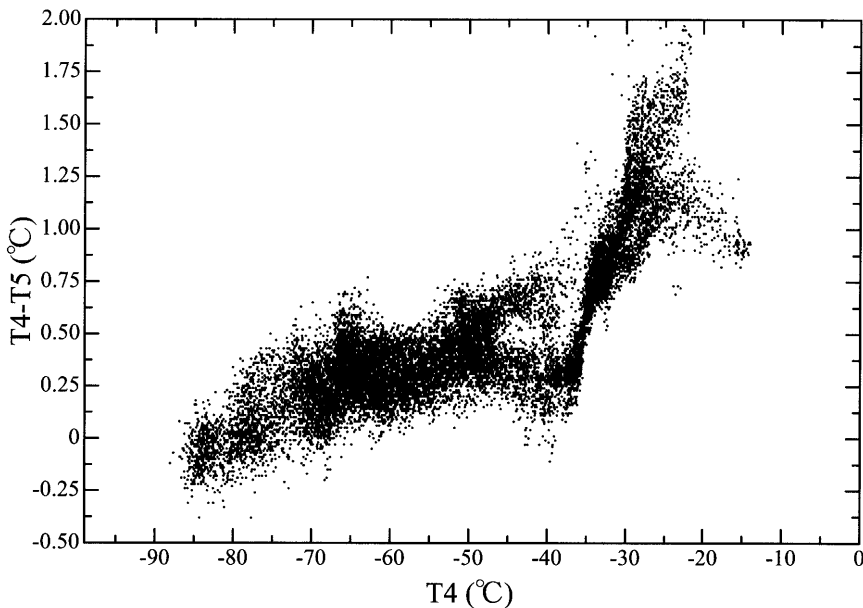

Fig. 3. *A scatter diagram of T4–T5 against T4 brightness temperature for extensive cloud free areas based on 5 passes (May 6, June 3, August 31, October 20, November 19, 1997). These areas were chosen by manual inspection using visible images. There is a tendency toward a positive spread in brightness temperature when T4 increases.*
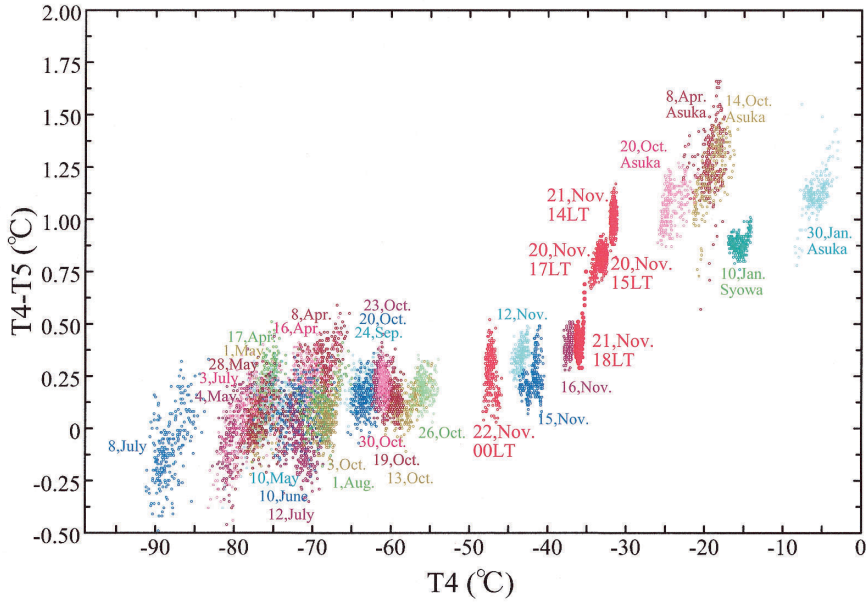
Fig. 4. A scatter diagram of T4–T5 in specific cloud free areas. The observation day is plotted with data. Each color is a different date. This distribution is approximately consistent with the distribution over extensive areas in Fig. 2.

the temperature at Dome Fuji Station and that at Syowa Station. Since there were no ground-based observation data near Asuka Station, cloud free conditions were assumed to exist from manual inspection of the images. Figure 4 shows much the same pattern as Fig. 3. In the range of T4 higher than $-30°C$, T4–T5 is distributed at the center on about $1°C$. These results lead to the conclusion that topography is not the cause of change in T4–T5.

The dependence of T4–T5 on T4 might be caused by absorption of water vapor in the atmosphere and/or the difference of emissivity at the snow and ice surface. In order to identify the effect on dependence on T4–T5 against T4 of water vapor in the atmosphere, calculations were done using surface meteorological and aerological observation data. The details of radiosonde data are described by JARE Data Reports (Hirasawa *et al.*, 1999). Although the measurement accuracy of the relative humidity under low temperature is perceived to be low (Bromwich, 1988), the mean monthly precipitable water at Dome Fuji Station and Syowa Station in Table 1 was calculated using original measured values. In January and February at Dome Fuji Station, no monthly means are shown in Table 1, since there were only few data. From Table 1, the precipitable water at Syowa Station is one order larger than that at Dome Fuji Station. In order to indicate the range of T4–T5 influenced by the difference water vapor amount contained in the atmosphere, we show the calculated value of T4–T5 from sonde data (black circles), and from values assuming the relative humidity in whole troposphere to be 99% (downward triangles) and 0% (upward triangles) using MODTRAN in Fig. 5. Figures 5a and 5b show results using values of each month at Dome Fuji Station and Syowa Station, respectively. The mean surface air temperature

Table 1. The mean monthly precipitable water at the two stations.
In January and February at Dome Fuji Station, no monthly
means existed.   The precipitable water at Syowa Station is one
order larger than that at Dome Fuji Station.

Month	Precipitable water ($\mathrm{g\,cm}^{-2}$)	
	Dome Fuji	Syowa
1	—	0.632
2	—	0.552
3	0.029	0.587
4	0.024	0.499
5	0.015	0.323
6	0.026	0.266
7	0.010	0.200
8	0.012	0.240
9	0.011	0.125
10	0.018	0.263
11	0.041	0.356
12	0.081	0.525

of the corresponding month is also shown (white circles).   For comparison to satellite data, this result is shown in Fig. 6 (double plots) with T4–T5 scatter diagram for the clear pixels.   Values of T4 at $-90°$C, $-80°$C and $-70°$C in Fig. 6 were calculated using the data only by changing the surface air temperature, using the temperature profile of August at Dome Fuji Station above the surface inversion layer.   Figure 6 shows that water vapor in the atmosphere has little influence on T4–T5 with T4 lower than $-25°$C.   In the case of the relative humidity set to 99%, T4–T5 increases greatly with T4 from $-25°$C by the effect of water vapor, and reaches about 0.75°C at 0°C (T4).

The T4–T5 that is given by the difference in the emissivity of snow and ice was also calculated using MODTRAN.   Many arguments have been made about the difference in emissivity of the snow and ice at different wavelengths in the infrared region; however, there is no satisfactory solution yet available (Hori *et al.*, 2001; Key *et al.*, 1997; Salisbury *et al.*, 1994; Key and Haefliger, 1992).   Key *et al.* (1997) calculated the emissivity at CH4 and CH5 following Dozier and Warren (1982), and showed that the difference in emissivity between CH4 and CH5 can be up to 0.0083.   In our study, the emissivity at 10.8 μm (CH4) was set to 1.00 and that at 12.0 μm (CH5) to 0.99, respectively, for all temperature regions since it is not far from the value of Key *et al.* (1997).   The result is shown in Fig. 6 (single plots).   We can see T4–T5 increase in all temperature ranges, and the difference in emissivity make the slight dependence of T4–T5 against T4 that T4–T5 increases with the increase of T4.   When T4 is lower than $-35°$C , this result agrees approximately with the satellite observations; however, when T4–T5 is higher than $-35°$C, the satellite observation data are higher than the calculated results.   This is difficult to explain only by the difference in the surface emissivity together with the atmospheric water vapor absorption.

We added the satellite data of T4–T5 against T4 in Dome Fuji Station at November 20, 15 LT, 17 LT, November 21, 14 LT, 18 LT, and November 20, 00 LT, 1997 in red to
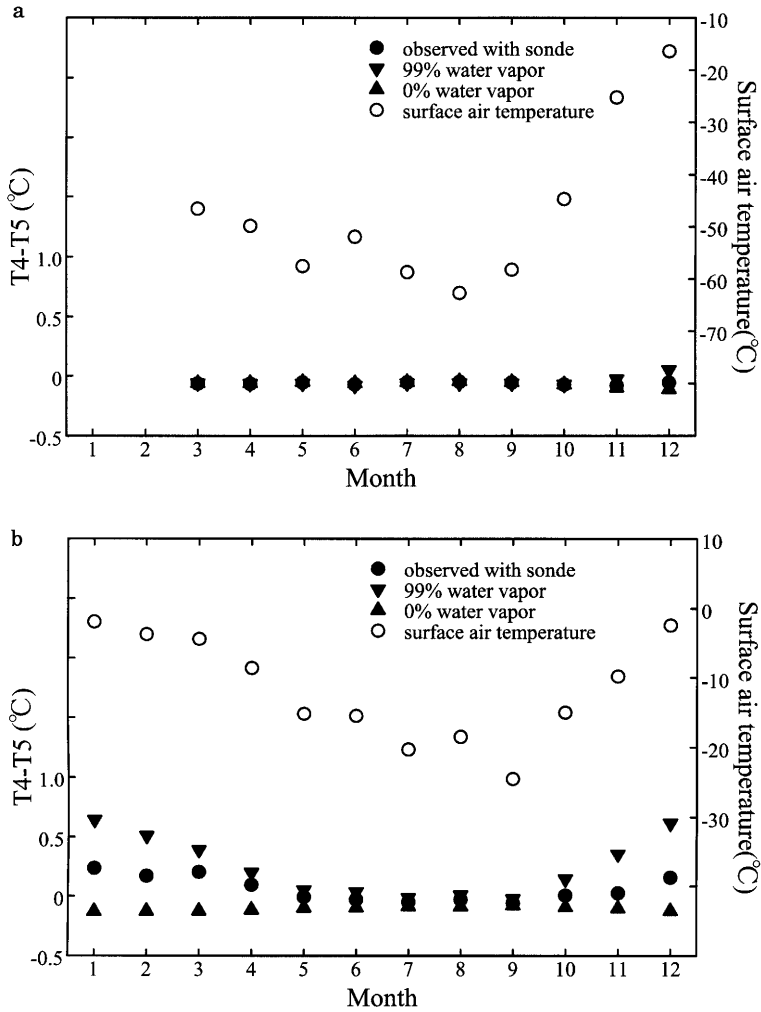
Fig. 5. *T4 and T5 calculated by MODTRAN based on monthly means of precipitable water in Table 1 and monthly means of temperature profile at Dome Fuji Station (a) and (b) Syowa Station (black circles). Downward triangles are the T4–T5 assuming the relative humidity of the whole troposphere to be 99%, and upward triangles are T4–T5 for 0%. White circles are mean surface temperatures in the corresponding months. In the colder area where only a small amount of water vapor can exist, T4–T5 is much smaller as opposed to the warmer area. Without water vapor, the absorption effect by ozone shows up slightly at a wavelength near 10 μm of the spectrum obtained by the CH4 detector at very low temperature; as a result, T4–T5 becomes negative.*

Fig. 4 to consider the series of changes in value of T4–T5 with change of time in this temperature range. From these data, we can see that T4–T5 is 0.2°C to 0.5°C at night at lower temperature; however, T4–T5 increases up to 1°C with the increases of T4 in the daytime when the temperature is higher. It is apparent that the change of T4–T5 responds to temperature change. A swift reduction can be seen in T4–T5 for 4 hours
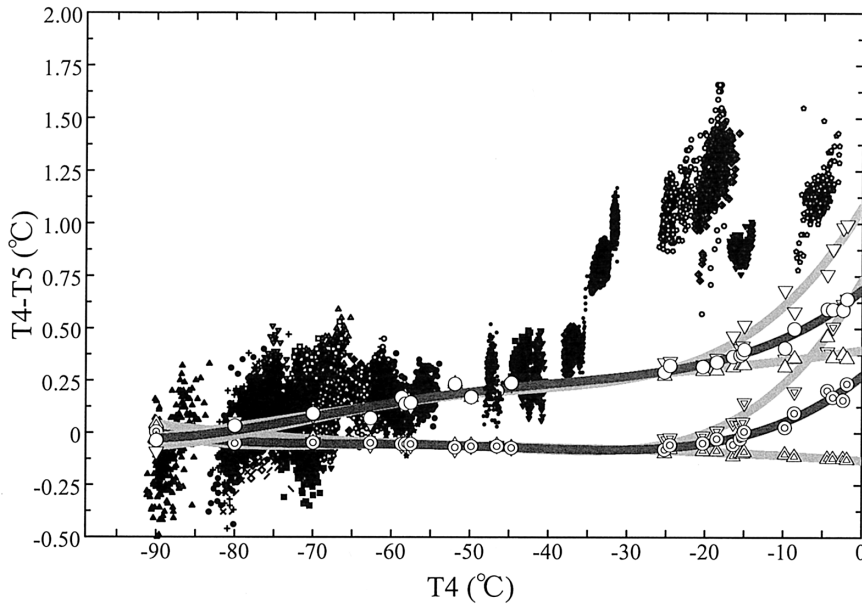
Fig. 6. *Calculation of T4–T5 based on absorption of water vapor with the identical surface emissivity for both channels (1.00; double plots), and that based on absorption of water vapor with the different surface emissivity (1.00 for CH4 and 0.99 for CH5; single plots).   Black lines are the least square fits to calculated T4–T5 values (circles) from sonde data.   Gray lines are fits to T4–T5 assuming the relative humidity to be 99% (downward triangles) and 0% (upward triangles), respectively. T4–T5 at −90°C, −80°C and −70°C (T4) in Fig. 6 was calculated with profiles in August at Dome Fuji Station assuming that only the surface temperature changes.   The amount of water vapor is insufficient to producing the observed T4–T5 in the lower temperature region.   The difference in surface emissivity causes T4–T5 to be positive at all temperatures.*

from 14 LT to 18 LT on November 21, suggesting quick response of T4–T5.   This change of T4–T5 could be caused by change of the optical property of snow particles around this temperature region.

Other factors affecting T4–T5 include dependence on the viewing angle from satellite (Yamanouchi *et al.*, 1987); however, the appear within a viewing angle of 20 degrees dependence did not clearly and is not discussed in the present study.

4.   Summary

A scatter diagram of satellite data indicates an increasing trend of T4–T5 versus T4 in the area of clear pixels irrespective of the topography.   At T4 around −80°C, T4–T5 can be seen around 0°C, and T4–T5 increases at a fixed rate with increase of T4 to −40°C.   At T4 from −40°C to −30°C, the rate of increase in T4–T5 becomes large; at T4 higher than about −30°C, T4–T5 is about 1°C.

The effects of water vapor in the atmosphere and of surface emissivity on T4–T5 were examined.   When the temperature of the near surface is high, a considerable amount of water vapor in the atmosphere can cause an increase in T4–T5.   In the lower

temperature region below $-40°C$ such as at Dome Fuji Station, even if water vapor is in saturation, it would be insufficient to produce the observed T4–T5.   On the other hand, the difference in surface emissivity can increase T4–T5 to a positive value at all temperatures, and can cause a slight dependence on T4 that the T4–T5 increases with increase of T4.   However, the estimated T4–T5 deviates from T4–T5 of satellite observation at higher temperature.   Both atmospheric water vapor and difference of emissivity together cannot explain the sudden increase of temperature dependence of T4–T5 around $-35°C$, seen in satellite data.   It is suggested that the sharp shift of T4–T5 around $-35°C$ is caused by the change in optical properties of snow particles with change in snow temperature.

　　　We may, therefore, reasonably conclude that there is a temperature dependence of T4–T5.   At very low temperature, the effect of difference of emissivity is dominant; at higher temperature, the effect of water vapor in the atmosphere becomes increasingly important.   However, both effects cannot completely explain T4–T5 at higher temperatures.   We need to examine the structural and optical changes of snow particles which might occur on the snow surface to arrive at a reliable conclusion.

Acknowledgments

References

Anderson, G.P., Kneizys, F.X., Chetwynd, J.H., Wang, J., Hoke, M.L., Rothman, L.S., Kimball, L.M. and McClatchey, R.A. (1995): FASCODE/MODTRAN/LOWTRAN: Past/Present/Future. 18th Annual Review Conference on Atmospheric Transmission Models, June, 6–8.

Bromwich, D.H. (1988): Snowfall in high southern latitudes. Rev. Geophys., **26**, 149–168.

Curry, J.A., Randall, D., Rossow, W.B. and Schramm, J.L. (1996): Overview of arctic cloud and radiation characteristics. J. Climate, **9**, 1731–1764.

Dozier, J. and Warren G.S. (1982): Effect of viewing angle on the infrared brightness temperature of snow. Water Resour. Res., **18**, 1424–1434.

Hirasawa, N., Hayashi, M., Kaneto, S. and Yamanouchi, T. (1999): Aerological sounding data at Dome Fuji Station in 1997. Data of Project on Atmospheric Circulation and Material Cycle in the Antarctic, Part 1. JARE Data Rep., **238**, 183 p.

Hori, M., Aoki, Te., Hachikubo, A. and Tanikawa, T. (2001): Dependence of spectral emissivity of snow upon quality in the thermal infrared region. The 24th Symposium on Polar Meteorology and Glaciology in Tokyo, Japan. Programme and Abstracts, 38.

Japan Meteorological Agency (1999): Antarctic Meteorological Data, 1996, ed by Japan Meteorological Agency, 1997, distributed on CD-ROM.

Key, J.R., Collins, J.B., Fowler, C. and Stone, R.S. (1997): High-Latitude Surface temperature estimates from thermal satellite data. Remote Sens. Environ., **61**, 302–309.

Key, J. and Haefliger, M. (1992): Arctic ice surface temperature retrieval from AVHRR thermal channels. J. Geophys. Res., **97**, 5885–5893.

NOAA (1988): Data Extraction and Calibration of TIROS-N/NOAA Radiometers. NOAA Technical Memorandum NESS 107-Rev. 1, ed. by W.G. Planet. 58 p.

NOAA (1998): NOAA Polar Orbiter Data Users Guide November 1998 Revision, ed. by K.B. Kidwell. 221 p.

Salisbury, J.W., D'Area, D.M. and Wald, A. (1994): Measurements of thermal infrared spectral reflectance of frost, snow, and ice. J. Geophys. Res., **99**, 24235–24240.

Yamanouchi, T. and Kawaguchi, S. (1984): Longwave radiation balance under a strong surface inversion in the katabatic wind zone, Antarctica. J. Geophys. Res., **89**, 11771–11778.

Yamanouchi, T., Suzuki, K. and Kawaguchi, S. (1987): Detection of clouds in Antarctica from infrared multispectral data of AVHRR. J. Meteorol. Soc. Jpn., **65**, 949–962.

Yamanouchi, T., Hirasawa, N., Kadosaki, G. and Hayashi, M. (2000): Evaluation of AVHRR cloud detection at Dome Fuji Station, Antarctica. Polar Meteorol. Glaciol., **14**, 110–116.